[NHN]$^+$ Hydrogen Bonding in Protonated 1,8-Bis(dimethylamino)-2,7-dimethoxynaphthalene. X-ray Diffraction, Infrared, and Theoretical ab Initio and DFT Studies

Valery A. Ozeryanskii,[†] Alexander F. Pozharskii,[†] Agnieszka J. Bieńko,[‡] Wanda Sawka-Dobrowolska,[‡] and Lucjan Sobczyk*[,‡]

Department of Organic Chlemistry, Rostov- State University, Zorge 7, 344090 Rostov-on-Don, Russia, and Faculty of Chemistry, University of Wrocław, F. Joliot-Curie 14, 50-383 Wrocław, Poland

Received: September 21, 2004

Structural (X-ray diffraction), infrared spectroscopic, and theoretical MP2 and DFT studies on the HBr and DBr adducts of 1,8-bis(dimethylamino)2,7-dimethoxynaphthalene ($(CH_3O)_2\cdot DMAN$) were performed. This particular proton sponge has been chosen for its strong basicity and display of the buttressing effect influencing the hydrogen bond dynamics and properties. The studies revealed a symmetric, planar DMAN·H$^+$ cation with a short (NHN)$^+$ hydrogen bond of 2.567(3) Å. The X-ray diffraction results suggest that the proton is in the central position in the bridge, while the calculations show two potential energy minima with the zero point energy level close to the top of the barrier. The infrared spectra display an (NHN)$^+$ band at 488 cm^{-1} and an (NDN)$^+$ band at 235 cm^{-1}, respectively. It gives the isotopic ratio of 2.08, the highest value reported to date. Such a result suggests a peculiar shape of the potential for the proton motion, characterized by an extremely high positive anharmonicity. The calculations reproduce this particular potential, yielding an ISR value displaying a very good agreement with the experimental one. The anharmonic frequencies, however, show the discrepancy between the observed and calculated transitions.

Introduction

The (NHN)$^+$ hydrogen bond in protonated "classical" proton sponge, 1,8-bis(dimethylamino)naphthalene (DMAN), has been a subject of several studies[1−6] concerning its basicity, X-ray structure, and NMR (^{1}H, ^{13}C, ^{15}N) and IR spectra. Despite many studies this problem still remains intriguing, probably due to the peculiar shape of the potential for the proton motion displaying the double minimum and low barrier. Several factors can affect the shape of such a potential. DMAN and its derivatives protonated by various acids can be used as model systems as they display the influence of both external and internal factors. The former are expressed in packing of the crystalline lattice whereas the latter act through steric and chemical effects of substituents in various positions on the naphthalene rings.

The crystallographic data (more than 40 structures of protonated DMAN with various counteranions have been reported[7]) show that the (NHN)$^+$ hydrogen bond length varies within a broad range of 2.54−2.64 Å. These results can be treated as an evidence of a soft interaction potential. For ca. 25% of DMAN·H$^+$ cations, symmetric (at least dynamically) bridges have been detected in the lattice. It seems obvious, that both the bridge length and symmetry of cations are related to the lattice packing. The short bridges are usually symmetric, but sometimes, as in the case of the protonation by trimethoxymethane,[8] longer bridges can be symmetric if the counteranions are disordered.

The IR spectra showed that for short bridges one observes the ν_{as}(NHN) absorption bands at extremely low frequencies in the region of 500 cm^{-1},[9] but the most intriguing is the anomalous isotope effect: the H/D isotopic ratio (ISR) can reach very high values, well above $\sqrt{2}$.[10] As the theoretical considerations show, the ISR value can be a sensitive probe for the potential shape and particularly the barrier height.[11] On the other hand, the recent intensive studies on NMR spectra, and particularly the H/D isotope effect, show that the double minimum potential in (NHN)$^+$ does exist in solution; the proton is attached to the one of nitrogen atoms jumping (or tunneling) with high frequency.[12−15] Especially important results, related directly to the subject of this paper have been reported by Perrin and Ohlta.[13]

The aim of this paper is the study of protonated (with HBr or DBr) 2,7-dimethoxy derivative of DMAN ($(CH_3O)_2\cdot DMAN$) by X-ray diffraction, IR spectra and quantum chemical calculations. This compound is interesting for two reasons. First, it is among the strongest bases in the family of DMAN derivatives.[14−18] Second, the 2,7-substitution causes the buttressing effect that has recently received growing attention.[19] It not only relates to a steric effect (interaction of the dimethoxy groups with CH$_3$ groups of dimethylamino moieties), but also to the charge distribution in the naphthalene ring and to the direct interaction via unconventional H-bonding between dimethylamino moieties with lone electron pairs of oxygen atoms in methoxy groups. Such bridges have recently been the subject of considerable interest in the literature.[20]

One should stress here that little is known to date regarding the structure and vibrational spectra of protonated DMAN derivatives. Only structures of 2,7-dichloro[21] and 2,7-dibromo derivatives[22] protonated by HBr have been published. These display symmetric NHN bridges, while in the case of 4-nitro[23] and 4-amino DMAN·H^{+7} the bridges are asymmetric with

---

* Corresponding author. E-mail: sobczyk@chem.uni.wroc.pl.
[†] University of Rostov.
[‡] University of Wrocław.

10.1021/jp040618l CCC: $30.25

unexpectedly low values of ISR. A detailed study on the potential shape has been performed for the 2,7-dibromo derivative using MP2 and DFT calculations.[22] This confirmed the existence of a double minimum potential with a low barrier and showed an unusual H/D isotope effect in IR spectra. The very short bridge and low ISR value obtained for 4-amino derivative[7] seems to be of great importance, as this suggests that the ISR value can yield important information about the shape of the potential.

Experimental and Computational Methods

2,7-$(CH_3O)_2$•DMAN was synthesized via a modification of the procedure described recently.[24] The salt of $(CH_3O)_2$•DMAN•HBr was prepared by adding 1 equiv of acid to an acetonitrile solution of the base, yielding colorless plates with mp 240−241 °C (dec, from MeCN). To obtain the deuterated salt $(CH_3O)_2$•DMAN•DBr, 0.2 mmol of 46% HBr was added to 2 mL of CD_3OD followed by 0.2 mmol of the dimethoxy DMAN. After the solvent was removed in vacuo, the residue was recrystallized from CD_3OD to give the deuterated complex as colorless plates. The estimated degree of deuteration was ca. 90%.

The X-ray diffraction studies were performed on a Kuma KM4 CCD and- KM4 four circle diffractometer equipped with an Oxford Cryosystem Cooler using graphite monochromated MoK_α radiation. The data were corrected for Lorentz and polarization effects, as well as for absorption. In the case of $(CH_3O)_2$•DMAN•DBr the correction for absorption was performed by using the empirical method included in the SHELXA program from the SHELXL-97 package.[25] For $(CH_3O)_2$•DMAN•HBr the analytical correction for absorption was applied.[26]

The structures were solved by direct methods with SHELXS-97[27] and refined by the full-matrix least-squares methods using the SHELXL-97 program.[25] Non-hydrogen atoms were refined with anisotropic thermal parameters. The H atoms in the $(CH_3O)_2$•DMAN•HBr molecule were found from difference synthesis and were refined isotropically. All H atoms in the crystal $(CH_3O)_2$•DMAN•DBr also were found in the difference synthesis and were included as fixed atoms in the final refinement, except for the D atom, which was refined.

The crystal data and structure refinements are summarized in Table 1. The XP package[28] was used to generate the molecular drawings.

The infrared spectra were recorded in Fluorolube (high-frequency region) or Nujol (low-frequency region) suspensions (CsI windows) using a Bruker IFS 113v FTIR spectrophotometer.

The full geometry optimization for the studied protonated sponge has been carried out at B3LYP and MP2 levels using double-ζ 6-31G(d,p) basis set with the Gaussian 98 program package.[29] After the optimization, the harmonic vibrational frequency calculations were performed to confirm the nature of the stationary point on the potential energy surface (PES) as a minimum. The potential energy curves were subsequently calculated allowing only the proton position in the hydrogen bridge to vary, while all the remaining geometry parameters were kept fixed at the corresponding theoretical equilibrium values. The potential energy curve has been obtained by scanning the potential energy surface along the NH coordinate, with NHN angle optimization at each point. Such an approach allowed us to take into account the NH stretch and NHN bend coupling to model the adiabatic process of the proton transfer.

TABLE 1: Crystal Data and Structure Refinement for HBr and DBr Salts of 1,8-Bis(dimethylamino)-2,7-dimethoxynaphthalene

empirical formula	$C_{16}H_{22}N_2O_2HBr$	$C_{16}H_{22}N_2O_2DBr$
fw	355.27	356.28
temp (K)	100(2)	100(2)
wavelength (Å)	0.710 73	0.710 73
cryst syst	monoclinic	monoclinic
space group	$C2/c$	$C2/c$
a (Å)	9.080(1)	9.027(1)
b (Å)	20.077(2)	19.991(2)
c (Å)	10.143(1)	10.084(1)
β (deg)	114.56(1)	114.47(1)
V (Å^3)	1681.9(3)	1656.2(3)
Z	4	4
D_c (Mg•m^{-3})	1.403	1.429
μ (mm^{-1})	2.450	2.488
F(000)	736	736
cryst size (mm)	0.26 × 0.21 × 0.11	0.60 × 0.40 × 0.20
θ range for data collcn (deg)	3.92−28.43	2.04−23.04
index ranges		
h	−12 to 11	0 to 9
k	−24 to 26	0 to 22
l	−12 to 13	−10 to 10
no. of reflcns collcd/unique	5478/1956	1191/1134
R(int)	0.0257	0.0206
abs cor	analytical	empirical
max and min transmission	0.761 and 0.569	0.762 and 0.343
data [I>2σ (I)]/params	1710/143	951/100
goodness-of-fit on F^2	1.056	1.073
R_1, wR_2 [$I > 2\sigma(I)$]	0.0266, 0.0566	0.0273, 0.0720
R_1, wR_2 indices (all data)	0.0367, 0.0595	0.0423, 0.0797
$\Delta\rho$ (e•Å^{-3})	0.274/−0.375	0.310/−0.334

As the harmonic approximation proved to be poor in predicting vibrational frequencies related to hydrogen bond, particularly in the case of proton stretch mode due to its strong anharmonicity as well as its coupling with the hydrogen stretch mode, we used the anharmonic approach to model the NH stretch mode. First, the ab initio energies were fitted with a sixth order polynomial V(r(HX)) and then the vibrational levels were calculated by solving a one-dimensional, vibrational, time-independent Schrödinger equation.[30] The vibrational Schrödinger equation was solved by variational principle using shifted Gaussian basis set consisting of 82 primitive Gaussians spanning from 0.3 to 2.3 Å.

Results and Discussion

X-ray Structure. The scheme presenting the structure of the HBr (DBr) adduct with $(CH_3O)_2$•DMAN is shown in Figure 1. The details related to the atom coordinates, bond lengths, bond angles, and other crystallographic data are deposited at the Cambridge Crystallographic Data Center (CCDC Nos. 2574424 and 257423). Here we would like to discuss some selected data connected with the main subject of this paper related to the $(NHN)^+$ hydrogen bond and its surroundings.

Taking into account the nitrogen and oxygen atoms as well as the Br^- anion as a base of construction, the system is almost perfectly planar; the corresponding torsion angles are in the limits 179−180°. Table 2 gathers data related to all hydrogen bonds including nonconventional bridges involving CH_3 groups. Selected geometry parameters for DMAN•H^+ cations along with the theoretical results are presented in Table 3.

The $(NHN)^+$ hydrogen bond length (2.567(3) Å) is rather typical for the symmetric DMAN•H^+ cations.[7] No geometrical isotope effect is observed within the experimental error. Compared to the 2,7-dibromo derivative,[22] which shows a particularly short hydrogen bridge, this bond is longer by 0.02 Å. In both cases, one is dealing with the buttressing substituents, albeit of different activity. In the dibromo derivative, relatively strong repulsion of the dimethylamino groups was shown to

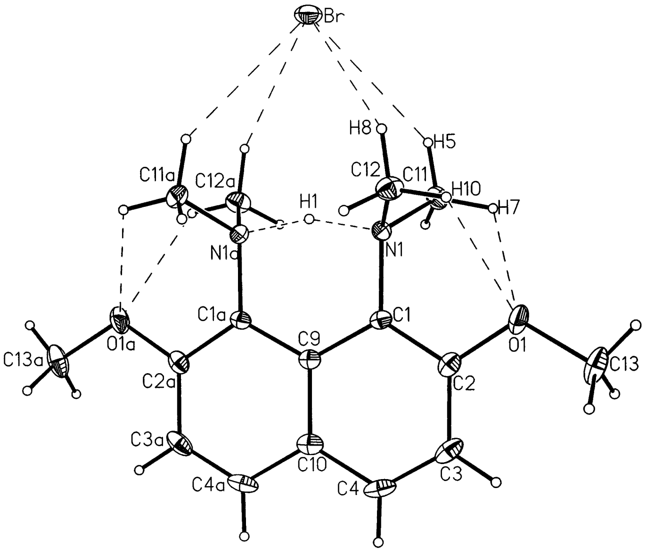

Figure 1. X-ray structure of the HBr salt of $(CH_3O)_2DMAN$ showing the 40% probability displacement ellipsoid with atom-numbering scheme. Symmetry code: (a) $-x + 1, y, -z + 0.5$.

TABLE 2: Hydrogen Bonds in HBr (A) and DBr (B) Salts of 1,8-Bis(dimethylamino)-2,7-dimethoxynaphthalene

	d(D−H···A)	d(D−H)	d(H···A)	d(D···A)	∠(DHA)
A	N(1)···H(1)···N(1)[a]	1.303(7)	1.303(7)	2.567(3)	160(3)
	C(11)−H(7)···O(1)	0.99(2)	2.42(2)	2.991(2)	115(2)
	C(12)−H(10)···O(1)	0.97(2)	2.43(2)	2.966(2)	115(2)
	C(11)−H(5)···Br	0.96(2)	2.99(2)	3.805(2)	144(2)
	C(12)−H(8)···Br	0.96(2)	2.96(2)	3.780(2)	144(2)
B	N(1)···D···N(1)[a]	1.302(11)	1.302(11)	2.561(5)	159(5)
	C(11)−H(7)···O(1)	0.96	2.40	2.971(4)	118
	C(12)−H(10)···O(1)	0.89	2.45	2.950(4)	116
	C(11)−H(5)···Br	0.95	2.98	3.790(3)	144
	C(12)−H(8)···Br	0.965	2.962	3.760(3)	141

[a] Symmetry code: (a) $-x + 1, y, -z + 0.5$.

TABLE 3: Selected Parameters for Protonated 1,8-Bis(dimethylamino)-2,7-dimethoxynaphthalene Calculated at B3LYP and MP2 Level with the 6−31G(d,p) Basis Set[a]

	calculated B3LYP	calculated MP2	experimental
C−O	1.359	1.367	1.368(2)
$N-C_1$	1.459	1.451	1.442(2)
$N-C_{11}$	1.476	1.464	1.490(2)
N−H	1.120	1.139	1.303(7)
$N_1 \cdots N_2$	2.600	2.567	2.567(3)
$C_{11}-H_7 \cdots O_1$	2.344	2.320	2.42(2)
$C_{12}-H_{10} \cdots O_1$	2.344	2.320	2.43(2)
$\angle N_1HN_2$	160.3	160.8	160(3)

[a] Bond lengths in angstroms, angles in degrees.

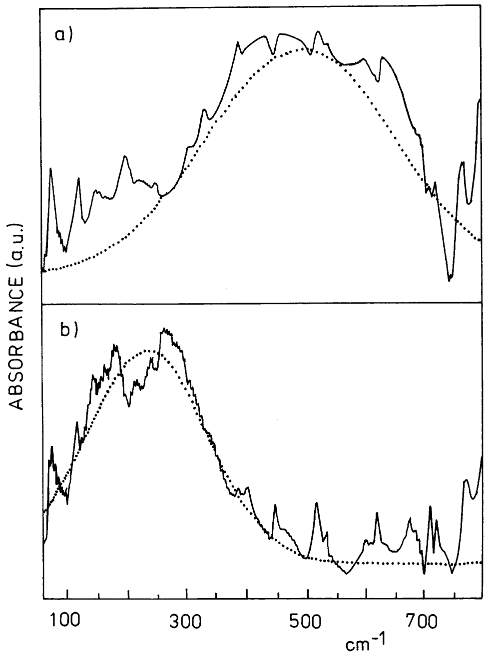

Figure 2. Separated infrared $(NHN)^+$ (a) and $(NDN)^+$ (b) bands fitted to Gaussian profiles (dotted curves).

TABLE 4: Positions (ν_{cg}), Half-widths (($\Delta\nu_{1/2}$) and Integrated Intensities (A) of NHN^+ and NDN^+ Bands in Protonated (deuterated) $(CH_3O)_2 \cdot DMAN$

	$\nu(NHN)^+$	$\nu(NDN)^+$
ν_{cg}/cm^{-1}	488 ± 5	235 ± 4
$\Delta\nu_{1/2}/cm^{-1}$	357 ± 6	214 ± 5
ISR ($\nu(NHN)^+/\nu(NDN)^+$)	2.08 ± 0.06	
$\Delta\nu_{1/2}(NHN)^+/\Delta\nu_{1/2}(NDN)^+$	1.67 ± 0.07	
$A(NHN)^+/A(NDN)^+$	1.35 ± 0.15	

cause shortening of the $(NHN)^+$ bridge owing to internal pressure. Analysis of the geometrical parameters for $(CH_3O)_2 \cdot DMAN \cdot H^+$ shows that the O(1)C(2)C(1) angle is smaller than O(1)C(2)C(3) (116.0(2) and 123.2(3)°, respectively). The factor causing this decrease is attraction between the *N*-methyl groups and the lone electron pairs of the oxygen atoms. This is well represented by the results in Table 2 related to the distances between the hydrogen atoms on the methyl groups and the oxygen atoms, which are significantly shorter than the sum of van der Waals radii. In contrast, the contacts between the methyl groups and Br^- are nearly equal to the sum of van der Waals radii. The most important result, however, is connected with the position of the hydrogen atom in the $(NHN)^+$ bridge. The structure refinement implies the central localization of this atom, at least in a dynamic meaning. This result differs from the data obtained previously for the dibromo derivative of DMAN, where two equivalent positions are occupied with the same probability.[22] As is explained in the discussion of the results, this arises from the zero point energy level being positioned close to the top of the barrier, and regardless of the temperature, there is only one maximum in the center of the $(NHN)^+$ bridge.

Infrared Spectrum. As our interest focuses mostly on the proton dynamics and properties of the $(NHN)^+$ bridge we will not discuss the vibrational spectrum in detail here. Such an analysis, based on IR and Raman spectra along with theoretical calculations, has been performed for several DMAN salts (see, for example, ref 31). In symmetrical $DMAN \cdot H^+$ cations one observes an intense band assigned to $\nu_{as}(NHN)^+$ vibration at extremely low frequencies, in the region around 500−600 cm^{-1}. The assignment of the broad intense IR band around 500 cm^{-1} in protonated proton sponges to the ν_{as}(NHN) stretching mode is based on the fact that the bending vibrations (usually coupled with the motion of other atoms) are located at much higher frequencies with rather small half-widths. Moreover it was shown[9] that, due to the Fermi resonance, one observes in many cases the Evans holes corresponding exactly to the frequencies of the deformation $\delta(NR_3)$ mode. Our experimental results for 1,8-bis(dimethylamino)-2,7-dimethoxynaphthalene are presented in Figure 2.

The experimental results relating to the infrared protonic NHN^+ and deuterated NDN^+ bands are also gathered in Table 4.

As the maximum level of deuteration attainable during preparation of the Nujol suspensions was ca. 75%, the infrared spectrum of this sample was that of a mixture of isotopomers

TABLE 5: Geometrical and Spectroscopic Characteristics of HBr Adducts with 2,7-X_2 Derivatives of DMAN

	∠C1C2X/deg	∠C3C2X/deg	D(N···N)/Å	ν(NHN)$^+$/cm^{-1}	ISR	ref
2,7-Br_2	124.7(2)	113.4(2)	2.547(3)	560	1.65	22
2,7-Cl_2	122.8(2)	115.4(2)	2.561(3)	530	1.80	21
2,7-$(OCH_3)_2$	116.0(2)	123.2(3)	2.567(3)	488	2.08	this paper

and so the separation of broad bands was accomplished by using the GRAMS program,[32] fitting to Gaussian profiles. The determination of the integrated intensities with sufficient accuracy was also not possible, therefore the analysis is limited to the intensity ratio of both bands.

The isotope effects presented in Table 4 proves that we are dealing with a peculiar potential for the proton motion. The most characteristic parameter is the ISR value, which is the highest obtained to date for short hydrogen bonds. Anomalously high values have been already reported for several protonated proton sponges, but only in one case it did reach a value over $\sqrt{2}$.[10] We are convinced that this is a strong evidence of an existing double minimum and low barrier potential. The potential shape resembles to some extent a rectangular character under these conditions.

We have managed to obtain relatively precise data for protonated DMAN with buttressing substituents in positions 2 and 7, namely di-Cl_2, di-Br_2, and di-$(CH_3O)_2$. The buttressing strain in the above compounds is characterized by the angles between the bonds formed by the substituent and the C−C bonds in the naphthalene ring. In all three cases we deal with a planar system of C_2 symmetry and the same counteranion Br^- located in the symmetry plane. The highest strain is observed for the di-Br_2 derivative. It is reduced for the di-Cl_2 compound while in the case of di-$(CH_3O)_2$ derivative the opposite effect is found. The OCH_3 and dimethylamino groups move closer together and the nonconventional C−H···O hydrogen bonds are observed. This is also reflected in the changes of the N···N bond lengths. As the symmetry is the same for all three derivatives and the same counteranion is used, we collected some data in Table 5 to compare the most important features for these systems.

Analysis of the data in Table 5 leads to the conclusion that we are dealing with hydrogen bonds in the critical region where small changes in geometry cause significant changes in the isotope effect represented by the ISR value.

The problem of other isotope effects on IR spectra of hydrogen bonded systems is still not completely solved in terms of the exact quantitative interpretation. This is particularly the case in relation to the half-width and intensity of protonic bands. As follows from the critical review[33] a number of different contributions should be taken into account. It seems that in our case the anomalous ISR effect is due to a “positive” anharmonicity as shown in ref 22, while less clear is the situation with respect to the isotope effects reflected in $\Delta\nu_{1/2}$ and A values. The isotopic A ratio equal to 1.35 may testify a lack of electrical anharmonicity.[34] The increase of the isotopic $\Delta\nu_{1/2}$ ratio compared to $\sqrt{2}$ is due to the coupling phenomena, connected with the mechanical anharmonicity,[35] but one cannot exclude the role of the Zundel polarizability[36] which should be very large in our case.

Calculations. In our previous paper,[22] we performed DFT (B3LYP) and MP2 calculations on the potential energy surface (PES) of Br_2·DMAN·H^+. The existence of a double minimum potential with low barrier was confirmed along with an unusual isotopic ratio (ISR). In this paper, we present the results for 1,8-bis(dimethylamino)-2,7-dimethoxynaphthalene [$(OCH_3)_2$·DMAN H^+] at both B3LYP and MP2 levels. As can be seen from Table 3, the geometry optimization shows a good agreement with the experimental results. We have not applied the Hartree−Fock method here as it showed inaccurate description for the previous calculations and proved to be inadequate for such systems due to the electron correlation neglection.

The calculations predict the length of N···N bridge in perfect agreement with the experimental bond length. Experimental results show that the hydrogen bond deviates from linearity, and this effect is well reproduced by theoretical calculations. This proves that nonlinearity is not caused by the lattice effects. As we have shown before, the best accuracy for the geometrical structure was obtained for the MP2 results as compared to the experimental values. This is consistent with previously drawn conclusions about the necessity of the electron correlation for the correct description of the anharmonic profiles in the hydrogen bonded complexes.[37] Thus, we concentrate only on the MP2 results in order to discuss the potential energy curve and the anharmonic frequencies for proton motion in NH(D)-N^+ bridge. For that purpose, Figure 3 shows the PES for ν(NHN)$^+$ normal mode calculations at the MP2/6-31G(d,p) level. The curve has been obtained by scanning the potential energy surface along NH coordinate with NHN angle optimization at each point. It allows consideration of coupling of the NH stretch and NHN bend to model the adiabatic process of the proton transfer. The anharmonic vibrational energy levels have been subsequently obtained by solving the one-dimensional Schrödinger equation.[30] The energy levels obtained for proton ν(NHN)$^+$ and deuteron ν(NDN)$^+$ motions are presented in Figure 3. The double minimum curve with a low barrier expected by experimental results has been confirmed by both DFT and MP2 calculations, which both showed the zero point energy to be slightly higher than the top of the barrier (17.1 and 10.1 cm^{-1} in the case of B3LYP and MP2, respectively). The results for both DFT and MP2 methods showed a similar tendency with a low barrier double minimum curve and a barrier of similar height.

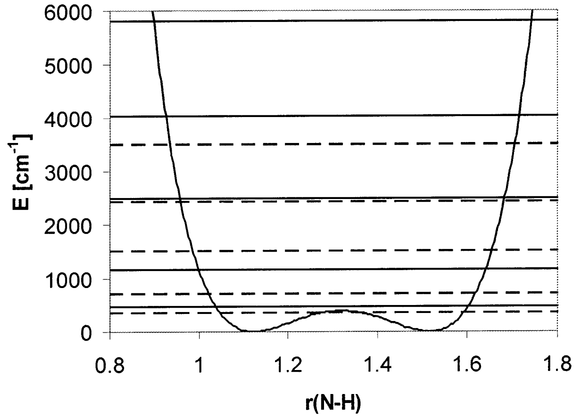

Figure 3. MP2 anharmonic potential energy levels for ν(NHN)$^+$ and ν(NDN)$^+$, with solid lines for protonic and dashed ones for deuteronic motion. Energy is given in cm^{-1}.

The theoretically predicted wavenumbers for the anharmonic fundamental band and four overtones are also presented in Table 6 along with B3LYP and MP2 results for comparison. The overtone wavenumbers show increasing energy differences confirming that we are dealing with unusual anharmonicity. This

TABLE 6: Calculated Energy Levels (in cm^{-1}) for Protonated and Deuterated 1,8-Bis(dimethylamino)-2,7-dimethoxynaphthalene

	$(OCH_3)_2DMAN{\cdot}H^+$		$(OCH_3)_2DMAN{\cdot}D^+$	
transition	B3LYP	MP2	B3LYP	MP2
0 → 1	665	692	331	352
0 → 2	1982	2014	1133	1156
0 → 3	3520	3568	2045	2079
0 → 4	5289	5349	3109	3152

TABLE 7: Theoretically Predicted Anharmonic $\nu(NHN^+)$ and $\nu(NDN^+)$ Frequencies (cm^{-1}) for 1,8-bis(dimethylamino)-2,7-dimethoxynaphthalene Compared to the Experimental Results, along with the ISR and Barrier Height Values

	ν(N−H−N)anh	ν(N−D-N)anh	ν(H)/ν(D)	barrier height cm^{-1}
DFT	665	331	2.01	475
MP2	692	352	1.97	462
expt	488	235	2.08	

phenomenon was shown in our previous paper[22] and is well reproduced by both levels of calculations used in this work. A comparison of theoretically predicted $\nu(NHN)^+$ and $\nu(NDN)^+$ frequencies (at B3LYP and MP2 levels) with experimental results along with isotopic ratio (ISR) and barrier height values are presented in Table 7. The fundamental mode $\nu(NH(D)N)^+$ is predicted by the DFT method at 663 cm^{-1} for $(CH_3O)_2$-DMANH$^+$ and at 331 cm^{-1} for its deuterated form. This gives the ISR ratio in an excellent agreement with experimental results (theoretical value = 2.01, experimental value = 2.08), and therefore confirms the unusually high ISR value, obtained for the first time experimentally. The MP2 method showed less accurate result for ISR but still the agreement with the experimental results is very good. The fundamental mode is slightly overestimated for both levels.

The discrepancy between the experimental and calculated stretching frequencies can be attributed most probably to the one-dimensional treatment. The full treatment, however, was too CPU (computer time) demanding and practically not possible to perform. Such a treatment means coupling not only with the NN motion but also with two other modes, namely NHN bond angle in-plane and out-of-plane modes. In the case of such a big system, using two-dimensional or mixed quantum classical treatment including additionally NN coordinate, with full atomic treatment is too CPU and memory demanding, in particular for the MP2 level of theory with a reasonable basis set.

Conclusions

The results of spectroscopic studies presented in this paper, particularly these related to the isotope effect, fit very well to the correlation proposed initially for OHO hydrogen bonds by Novak.[38] This correlation has been subsequently developed for NHN bridges.[10] It suggests that toward to the critical range of charge assisted hydrogen bonds, a sharp increase of the ISR value takes place, to significantly more than $\sqrt{2}$. One should expect particularly high values of ISR when the $\nu(NHN)^+$ band appears around 500 cm^{-1} as in the case of $(CH_3O)_2DMANH^+$.

It is difficult to conclude whether further shortening of the NHN bridge is possible in the case of DMAN derivatives. Such an effect, however, has been observed by Alder in protonated 1,6-diazabicyclo[4.4.4]tetradecane for which the N···N bond length is 2.526(3) Å.[39,40] This is an unique example of a symmetric single minimum potential $[NHN]^+$ hydrogen bond, confirmed by the H/D NMR isotope effect. The IR spectrum shows the absorption below 2000 cm^{-1}, similar to numerous analogues of symmetric and close to symmetric $[OHO]^+$ bridges.[41] For ISR values higher than $\sqrt{2}$, however, such high wavenumbers have never been recorded for $[OHO]^+$ absorption as compared to those for $[NHN]^+$. The difference can possibly be explained based on the theoretical analysis performed by Scheiner[11,42−43] who has shown substantial differences in the charge distribution for $[OHO]^+$ and $[NHN]^+$. Thus, the proton located in the midpoint along the O···O axis is more deshielded than that along the corresponding N···N one (N···N is about 0.1 Å longer). As a consequence the oxygen atoms lose less electron density than do the nitrogen atoms. This is also well reflected in the ^1H NMR chemical shift for strongest $[OHO]^+$ and $[NHN]^+$ bridges. The highest δ ^1H value for protonated proton sponge reported so far reached 20.33 ppm (just for 2,7-dibromo derivative), while in the case of homoconjugated (OHO) ions the ^1H chemical shift can exceed 25 ppm.[44]

The conclusions formulated in this paper seem to be in a full agreement with recently published data related to the shortest intramolecular OH···O hydrogen bonding in 4-cyano-2,2,6,6-tetramethyl-3,5-heptanedione.[45] Although neutron diffraction measurements show a central localization of the bridge proton (with elongated thermal ellipsoid) dynamical features of the system reflected in inelastic neutron scattering indicate a double minimum potential with very low barrier. Simultaneously, which seems to be very important, the mode assigned to the proton vibrations along the bridge is characterized by a frequency of 371 cm^{-1}. The analogy with the system studied in this paper is well visible. Therefore, it is not peculiar that the X-ray diffraction results in our case show a central position for the hydrogen atom while the IR data and calculations univocally show a double minimum potential for the proton motion.

Acknowledgment. Thanks to Dr. Krzysztof Mierzwicki, Dr. Dariusz Bieńko, and Dr. Bogusława Czamik-Matusewicz for valuable suggestions and stimulating discussions. Dr. Charles M. Gordon is gratefully acknowledged for reading and commenting the manuscript. The authors acknowledge the Wrocław and Poznań Supercomputer Centers for providing computer time. V.A.O. and A.F.P. are grateful for support from the Russian Foundation for Basic Research through Grant No. RFBR 02-03-32080.

References and Notes

(1) Pozharskii, A. F. *Usp. Khim.* **1998**, *67*, 3.
(2) Alder, R. W. *Chem. Rev.* **1989**, *89*, 1215.
(3) Hibbert, F.; Emsley, J. *Adv. Phys. Org. Chem.* **1990**, *26*, *255*.
(4) Staab, H. A.; Saupe, T. *Angew. Chem., Int. Ed. Engl.* **1988**, *27*, 865.
(5) Llamas-Saiz, A. L.; Foces-Foces, C.; Elguero, J. *J. Mol. Struct.* **1994**, *328*, 297.
(6) Perrin, C. L.; Nielson, J. B. *Annu. Rev. Phys. Chem.* **1997**, *48*, 514.
(7) Ozeryanskii, V. A.; Pozharskii, A. F.; Głowiak, T.; Majerz, I.; Sobczyk, L.; Grech, E.; Nowicka-Scheibe, J. *J. Mol. Struct.* **2002**, *607*, 1.
(8) Woźniak, K.; Raczyńska, E. D.; Korybut-Daszkiewicz, B. *Isr. J. Chem.* **1999**, *39*, 245.
(9) Brzeziński, B.; Głowiak, T.; Grech, E.; Malarski, Z.; Sobczyk, L. *Croat. Chem. Acta* **1992**, *65*, 101.
(10) Grech, E.; Malarski, Z.; Sobczyk, L. *Chem. Phys. Lett.* **1986**, *128*, 259.
(11) Scheiner, S. *J. Phys. Chem.* **1982**, *86*, 376.
(12) Grech, E.; Klimkiewicz, J.; Nowicka-Scheibe, J.; Pietrzak, M.; Schilf, W.; Pozharskii, A. F.; Ozeryanskii, V. A.; Bolwig, S.; Abildgaard, S.; Hansen, P. E. *J. Mol. Struct.* **2002**, *615*, 121.
(13) Perrin, C. L.; Ohta, B. K. *J. Am. Chem. Soc.* **2001**, *123*, 6520.
(14) Pietrzak, M.; Stefaniak, L.; Pozharskii, A. F.; Ozeryanskii, A.; Nowicka-Scheibe, J.; Grech, E.; Webb, G. A. *J. Phys. Org. Chem.* **2000**, *13*, 35.

(15) Pozharskii, A. F.; Ozeryanskii, V. A. *Russ. Chem. Bull.* **1998**, *47*, 66.

(16) Hibbert, F.; Hunte, K. P. P. *J. Chem. Soc. Perkin Trans 2* **1983**, 1895.

(17) Kirsch, A.; Krieger, C.; Staab, H. A.; Neugebauer, F. A. *Tetrahedron Lett.* **1994**, *35*, 8365.

(18) Peräkylä, M. *J. Org. Chem.* **1996**, *61*, 7420.

(19) Pozharskii, A. F.; Ryabtsova, O. V.; Ozeryanskii, V. A.; Degtyarev, A. V.; Kazheva, O. N.; Alexandrov, G. G.; Dyachenko, O. A. *J. Org. Chem.* **2003**, *68*, 10109.

(20) Desiraju, G. R.; Steiner, T. *The weak hydrogen bond in structural chemistry and biology*; Oxford University Press Inc.: New York, 1999.

(21) Głowiak, T.; Majerz, I.; Malarski, Z.; Sobczyk, L.; Pozharskii, A. F.; Ozeryanskii, V. A.; Grech, E. *J. Phys. Org. Chem.* **1999**, *12*, 895.

(22) Bieńko, A. J.; Latajka, Z.; Sawka-Dobrowolska, W.; Sobczyk, L.; Ozeryanskii, V. A.; Pozharskii, A. F.; Grech, E.; Nowicka-Scheibe, J. *J. Chem. Phys.* **2003**, *119*, 4313.

(23) Pozharskii, A. F.; Kuz'menko, V. V.; Aleksandrov, G. G.; Dmitrienko, D. V. *Zh. Org. Khim.* **1995**, *31*, 570.

(24) Ozeryanskii, V. A.; Sorokin, V. I.; Pozharskii, A. F. *Russ. Chem. Bull.* **2004**, *53*, 404.

(25) Scheldrick, G. M. SHELXL-97, Program for the Refinement Structure, University of Götingen, Germany, 1997.

(26) Kuma Diffraction Software, Crys. Alis CCD, Alis Red 1.66.

(27) Scheldrick, G. M. SHELXS-97, Program for Solution of Crystal Structure Refinement, University of Götingen, Germany, 1997.

(28) SHELXTL Version 5.10, Bruker AXS. Inc. Madison, Wisconsin, USA.

(29) Frisch, M. J.; Trucks, G. W.; Schlegel, H. B.; et al. Gaussian 98, Rev A9, Gaussian Inc.: Pittsburgh, PA, 1998.

(30) Stare, J.; Mavri, J. *Comput. Phys. Commun.* **2002**, *143*, 222.

(31) Baran, J.; Pawlukojc, A.; Majerz, I.; Malarski, Z.; Sobczyk, L.; Grech, E. *Spectrochim. Acta* **2002**, *A56*, 1801.

(32) GRAMS/386, User's Guide, Galactic Industries Corporations.

(33) Mielke, Z.; Sobczyk, L. *Vibrational isotope effects in hydrogen bonds, in: Isotope effects in biology and chemistry*; Kohen, A., Limbach, H.-H.; Eds.; M. Dekker: New York, in press.

(34) Marechal, E.; Bratos, S. *J. Chem. Phys.* **1978**, *68*, 1825.

(35) Henrie-Rousseau, O.; Blaise, P.; Chamma, D. *Adv. Chem. Phys.* **2002**, *121*, 241.

(36) Zundel, G. *Adv. Chem. Phys.* **2000**, *111*, 1.

(37) Biczysko, M.; Latajka, Z. *J. Phys. Chem.* **2002**, *106*, 3107.

(38) Novak, A. *Struct. Bonding* **1974**, *18*, 177.

(39) Alder, R. W.; Orpen, A. G.; Sessions, R. B. *J. Chem. Soc., Chem. Commun.* **1983**, 999.

(40) Alder, R. W.; Moss, R. E.; Sessions, R. B. *J. Chem. Soc., Chem. Commun.* **1983**, 1000.

(41) Kreevoy, M. M.; Marimanikkuppam, S.; Young, V. G., Jr.; Baran, J.; Szafran, M.; Schultz, A. J.; Trouw, F. *Ber. Bunsen-Ges. Phys. Chem.* **1998**, *103*, 370.

(42) Scheiner, S. *J. Am. Chem. Soc.* **1981**, *103*, 2169.

(43) Scheiner, S. *J. Chem. Phys.* **1982**, *77*, 4039.

(44) McDermott, A.; Ridenour, C. F. *Encyclopedia of NMR*; J. Wiley: Sussex, U.K., 1996.

(45) Belot, J. A.; Clark, J.; Cowan, J. A.; Harbison, G. S.; Kolesnikov, A. I.; Kye, Y.-S.; Schultz, A. J.; Silvernail, C.; Zhao, X. *J. Phys. Chem. B* **2004**, *108*, 6922.